iScience

CellPress
OPEN ACCESS

Article

Discordant interactions between YAP1 and polycomb group protein SCML2 determine cell fate

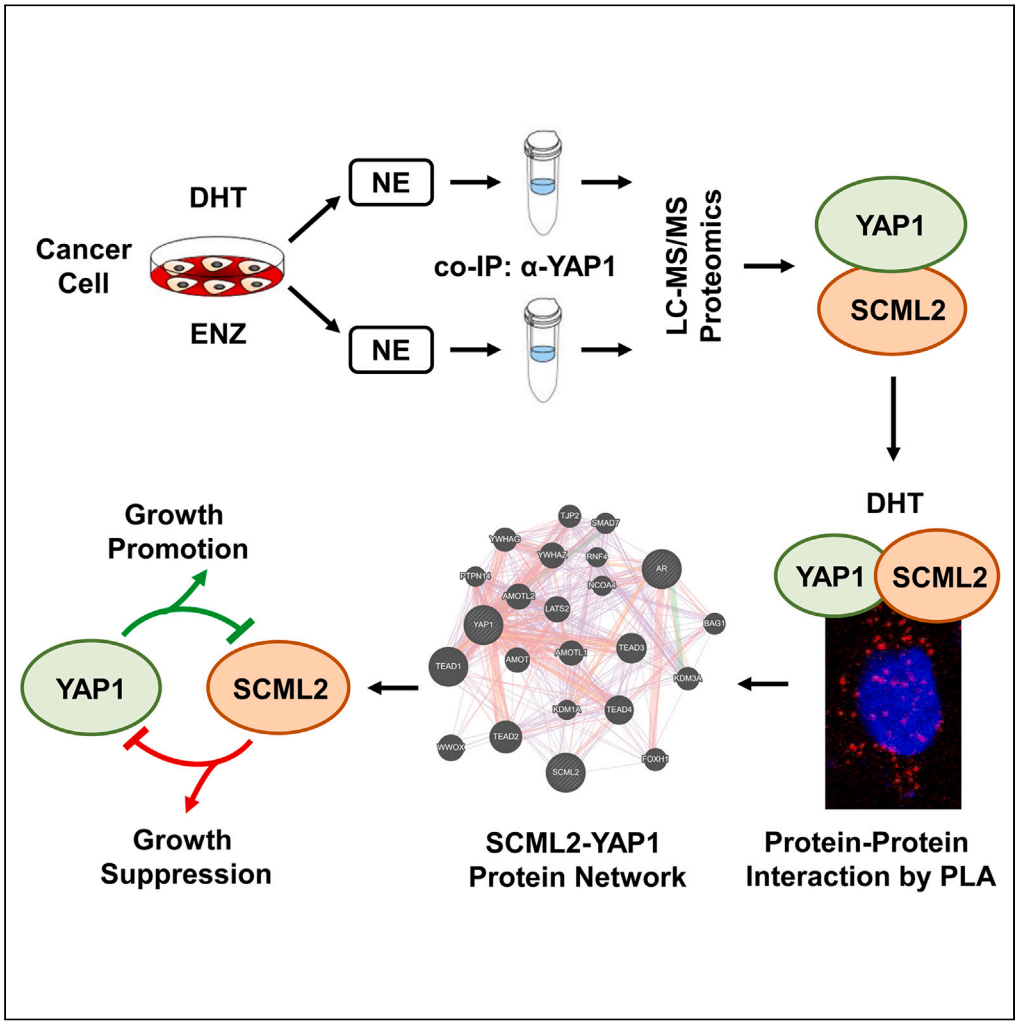

Ava M. Boston, Abdulrahman M. Dwead, Marwah M. Al-Mathkour, ..., Qiang Zhang, Guangdi Wang, Bekir Cinar

bcinar@cau.edu

Highlights

Polycomb repressive protein SCML2 biochemically and functionally interacts with YAP1

SCML2 depletion alters cell growth in response to streoid hormone androgen signaling

SCML2 and YAP1 inversely modulate H3K27me3 and H2AK119Ub chromatin modifications

Cooperative SCML2 and YAP1 signaling regulates cell growth and cell survival

Boston et al., iScience 26, 107964
October 20, 2023
https://doi.org/10.1016/j.isci.2023.107964

iScience

CellPress
OPEN ACCESS

Article

Discordant interactions between YAP1 and polycomb group protein SCML2 determine cell fate

Ava M. Boston,[1,3] Abdulrahman M. Dwead,[1,3] Marwah M. Al-Mathkour,[1,3] Kezhan Khazaw,[1] Jin Zou,[1] Qiang Zhang,[2] Guangdi Wang,[2] and Bekir Cinar[1,4,*]

SUMMARY

The Polycomb group protein SCML2 and the transcriptional cofactor YAP1 regulate diverse cellular biology, including stem cell maintenance, developmental processes, and gene regulation in mammals and flies. However, their molecular and functional interactions are unknown. Here, we show that SCML2 interacts with YAP1, as revealed by immunological assays and mass spectroscopy. We have demonstrated that the steroid hormone androgen regulates the interaction of SCML2 with YAP1 in human tumor cell models. Our proximity ligation assay and GST pulldown showed that SCML2 and YAP1 physically interacted with each other. Silencing SCML2 by RNAi changed the growth behaviors of cells in response to androgen signaling. Mechanistically, this phenomenon is attributed to the interplay between distinct chromatin modifications and transcriptional programs, likely coordinated by the opposing SCML2 and YAP1 activity. These findings suggest that YAP1 and SCML2 cooperate to regulate cell growth, cell survival, and tumor biology downstream of steroid hormones.

INTRODUCTION

The Polycomb group (PcG) proteins are well-characterized epigenetic regulators of developmental genes in higher eukaryotes.[1,2] Polycomb repressive complexes 1 and 2 (PRC1 and PRC2) are the canonical chromatin modifiers.[3,4] SCML2 (sex comb on midleg like-2) gene on chromosome Xp22 suppresses gene expression during development in flies and mammals. SCML2 is a subunit of the canonical PRC1, which controls differentiation and preserves the stem cell features.[5] SCML2 and its homologs SCMH1, SCML1, SFMBT1, and SFMBT2 are an ortholog of the Drosophila SCM (sex comb on midleg) and SFMBT family proteins.[6–10] SCML2 regulates gene expression by orchestrating the PRC1 and PRC2.[11] Also, SCML2 is identified as a germline-specific gene and thus plays a critical role in maintaining homeotic genes in the germline or germ cells.[11] Germ cells such as spermatogonia, spermatocytes, and round spermatids express high levels of SCML2,[12] and silencing SCML2 caused defects in spermatogenesis and reduced sperm production in male mice.[13]

SCML2 has a conserved domain architecture like the SCM protein family. SCML2 has two MBT (malignant brain tumor) repeats located in the N-terminus, an SLED (SCM-like embedded domain, also known as DUF3588) domain, and a sterile alpha motif (SAM) in the C-terminus. The molecular and functional studies have demonstrated that the MBT repeats mediate the binding of SMCL2 to a monomethylated lysine residue on histones.[14,15] In addition, Bonasio et al. identified SCML2 as an RNA-binding protein (RBP).[16] In that study, SCML2 was demonstrated to interact with RNA through its RNA-binding region (RBR) located between MBT and SLED domains, resulting in chromatin recruitment and suppression of its target genes.[16] Although it is less clear, the SLED domain might mediate the binding of SCML2 to double-stranded DNA in a sequence-specific manner so that SCML2 may regulate the PRC1-mediated gene silencing.[5] Furthermore, the SLED domain could facilitate the interaction of SCML2 with PRC1.[5] Finally, the SAM domain could also facilitate the binding of SCML2 to the PRC1.[3] Thus, having multiple functional protein domains may account for its diverse cellular functions.

The SCM proteins act as potent transcriptional suppressors upon association with chromatin.[17] SCML2 regulates its target gene expression by multiple mechanisms.[18] SCML2 binds to chromatin with the modification of trimethylated histone H3 on lysine 27 (H3K27me3),[13] a gene-suppressive histone mark catalyzed by the histone methyl transferase EZH2 (enhancer of zeste homolog 2), which a catalytic subunit of the PRC2. In addition to the H3K27me3-mediated chromatin binding, SCML2 interacts with chromatin through monoubiquitinated-histone H2A at the target sites.[19,20] For example, RNF2, a ubiquitin E3-ligase component of the PRC1, monoubiquitylates H2A on lysine 119 (H2AK119Ub), leading to transcriptional silencing and X-inactivation.[21,22] Besides, a study by Adams et al. showed that SCML2 interacts with the DNA damage protein RNF8 E3-ubiquitin ligase to control gene expression by regulating the H2A ubiquitination and H3K27

[1]Department of Biological Sciences, Center for Cancer Research and Therapeutic Development, Clark Atlanta University, Atlanta, GA, USA
[2]Department of Chemistry, Xavier University of Louisiana, New Orleans, LA, USA
[3]These authors contributed equally
[4]Lead contact
*Correspondence: bcinar@cau.edu
https://doi.org/10.1016/j.isci.2023.107964

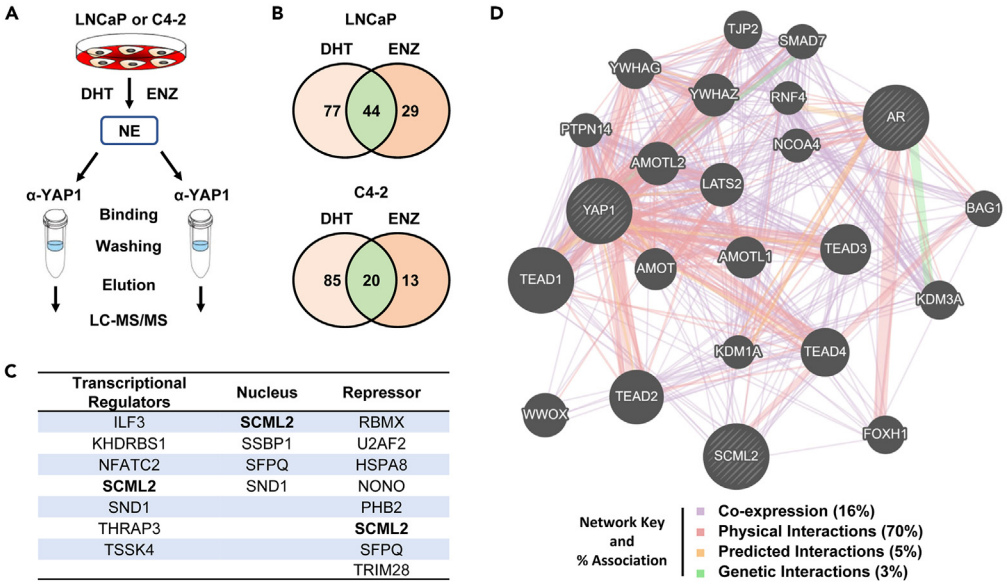

Figure 1. Strategies to identify SCML2 as a YAP1-associated protein

(A) Diagram showing the proteomics analysis of YAP1-associated proteins from the nuclear extracts (NE) from LNCaP and C4-2 cells after treatment with dihydrotestosterone (DHT, 10 nM) or enzalutamide (ENZ, 20 μM) for 16h in DCC (dextran-coded charcoal-stripped) serum-fed conditions.

(B) Venn diagram shows the YAP1 interacting proteins in LNCaP and C4-2 cells.

(C) The table shows YAP1 interacting proteins that are transcriptional regulators, localize to the nucleus, and function as repressors.

(D) YAP1 protein network in connection with SCML2 and AR. Protein networks were constructed using the GeneMania web portal.

acetylation.[23] Also, SCML2 was associated with chromatin by binding to phosphorylated Histone H2A.X.[24] Moreover, SCML2 interacted with the SWI/SNF (switching defective/sucrose non-fermenting) complex to regulate gene transcription.[20] In that study, the author showed that SCML2 interacted with BRG1 of the SWI/SNF complex in spermatocytes and modulated gene transcription during meiosis.

The YAP1 (yes-associated protein 1) or its close paralog WWTR1 (aliase TAZ) are transcriptional cofactors that activate or repress gene expression, mainly downstream of the Hippo pathway.[25–30] The Hippo pathway controls cell-cell interaction and organ size by suppressing cell proliferation and inducing apoptosis through restricting YAP1 activity.[31,32] The present study investigated the biochemical and functional link between YAP1 and SCML2 in the androgen receptor (AR)-positive LNCaP and C4-2 cell models. Using proteomics approaches, we identified SCML2 from the nuclear YAP1 protein complexes of LNCaP and C4-2 cells. Our data demonstrate that steroid hormone androgen signaling regulates the subcellular localization and interaction of SCML2 with YAP1. In addition, our genetic silencing showed that SCML2 and YAP1 reciprocally regulate each other's expression and activity, indicating a functional antagonism between YAP1 and SCML2. Silencing SCML2 in LNCaP resulted in androgen-independent cell growth and reduced the anti-growth efficacy of enzalutamide (ENZ), whereas silencing SCML2 in C4-2 had the opposite effect. Moreover, our data revealed that SCML2 and YAP1 oppositely regulated gene-suppressive H3K27me3 and H2AK119Ub histone marks. Furthermore, we have found that many SCML2 and YAP1 target genes overlap. These observations indicate that molecular and functional links between YAP1 and SCML2 are critical for cell growth and androgen-mediated oncogenesis.

RESULTS

SCML2 interacts with the YAP1 protein complex

Our previous work showed that steroid hormone androgens regulate YAP1 nuclear localization and its protein-protein interaction with the AR.[33,34] To gain further insights into the biology of YAP1 downstream of androgens, we wanted to identify the nuclear YAP1 interacting proteins. We took stepwise approaches to accomplish this goal. First, we generated the IgG control and the YAP1 antibody-crosslinked protein A/G agarose columns. Second, we isolated the nuclear fractions from the human androgen-dependent (AD) LNCaP and its androgen-independent (AI) C4-2 subline under steady-state conditions and incubated them with the IgG and the YAP1 antibody column. Third, the bound proteins were eluted after extensive washing, and the presence of YAP1 was analyzed by western blotting (Figure S1A). The results showed that the YAP1 protein was successfully captured by and eluted from the YAP1 column (Figure S1B). The observation is specific because elutes from the IgG column or flow-through lacked the YAP1 signal (Figure S1B). The human prostate tumor cell lines, LNCaP and C4-2, were ideal for this study because these cells are genetically related but phenotypically different because they respond to androgen hormone signaling *ex vivo* and *in vivo* differentially.[35] Also, androgens differentially regulate YAP1 and AR interaction in these cells.[34]

Next, the nuclear fractions obtained from LNCaP and C4-2 cells after treatment with androgen (DHT) or anti-androgen ENZ were incubated with the YAP1 antibody column. Following extensive washing, proteins were eluted and analyzed by liquid chromatography (LC) coupled to MS/MS (mass spectroscopy) (Figure 1A). LC-MS/MS proteomics identified 121 and 73 YAP1 interacting proteins from LNCaP cells

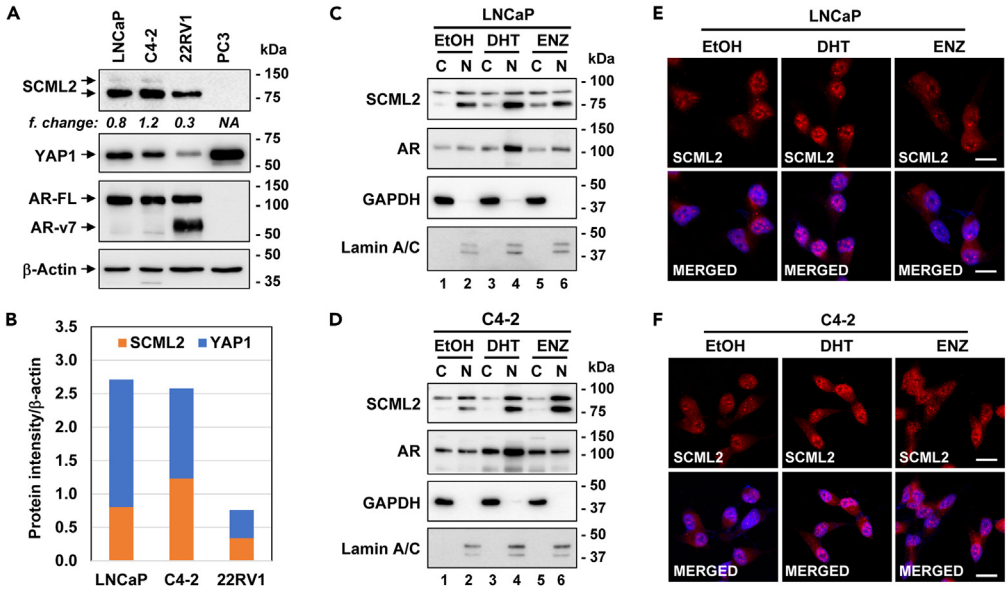

Figure 2. Androgen regulates the SCML2 subcellular localization

(A) Immunoreactivity of SCML2 and YAP1 proteins total cell lysates isolated from the AR-positive and the AR-negative human cell lines grown under steady-state conditions. SCML2 blot was generated using SCML2 (G1) mouse monoclonal antibody. The beta-actin blot was included as a loading control.

(B) Quantification of the SCML2 and YAP1 blots normalized to the beta-actin.

(C and D) Western blots of SCML2 and AR in LNCaP and C4-2 cells. SCML2 blot was generated with the SCML2 (C-7) antibody. GAPDH and Lamin A/B blots were used for cytoplasmic (C) and nuclear (N) protein markers, respectively.

(E and F) Immunofluorescence (IF) imaging of SCML2 in LNCaP and C4-2 cells. LNCaP and C4-2 cells were treated with ethanol (EtOH) vehicle, DHT (dihydrotestosterone, 10 nM), and ENZ (enzalutamide, 20 μM) 16h in DCC serum-fed conditions. IF data were generated using SCML2 (G1) antibody. Data are represented as mean ± SEM of three independent experiments. The size bar: 10 μm.

in DHT or ENZ-treated conditions, respectively, and 44 proteins overlapped between treatments (Figure 1B, LNCaP). ENZ exposure reduced the number of YAP1 interacting proteins, suggesting that the observation is specific, and DHT exposure modulated YAP1-associated protein complexes. Similarly, the number of YAP1-associated proteins in C4-2 under the same conditions was 105 for DHT and 33 for ENZ treatment, and 20 proteins overlapped between DHT and ENZ treatment (Figure 1B, C4-2). Furthermore, our functional annotation clustering showed that YAP1-associated proteins were enriched for diverse cellular pathways, including RNA transport, RNA processing, RNA translation, post-transcriptional regulation, protein folding, and metabolism (Figures S2A and S2B, Tables S1, and S2).

YAP1 regulates the expression of several genes involved in diverse cell biology, including cell growth, cell survival, cell differentiation, cell transformation, carcinogenesis, and metastasis.[36] Therefore, we selected SCML2 to establish its interaction with YAP1 because it acts as a transcriptional regulator and is a nuclear-resident protein (Figure 1C). Also, SCML2 shared similar cellular activities with YAP1, such as regulating gene expression, controlling developmental processes, stemness, and cell growth.[11,12,20,37–39] Besides, our protein network analysis showed an apparent link between SCML2 and YAP1, and SCML2 interacts with other proteins within the YAP1 protein network (Figure 1D).

SCML2 differentially responds to androgen signaling

To identify the cell models that allow us to study the interaction between YAP1 and SCML2, we assessed the levels of SCML2 protein expression along with YAP1 and AR in the AR-positive LNCaP, C4-2, and 22Rv1 cells as well as in the AR-negative PC3 cell. Notably, LNCaP, C4-2, and 22Rv1 but not PC3 expressed SCML2 (Figures 2A and 2B). SCML2 has two isoforms: SCML2A, the full-length (FL) version, and SCML2B, a C-terminal truncation generated by alternative splicing. Both isoforms are predominantly nuclear; SCML2A is usually enriched in the chromatin fraction, while SCML2B is increased in the soluble nuclear fraction.[16] SCML2A was detected in total cell lysate (Figure 2A, upper band) compared to SCML2B (Figure 2A, lower band). Therefore, we will use SCML2 in the rest of the manuscript. Quantification of the blot showed that C4-2 cells expressed 1.5-fold elevated SCML2 protein compared to the LNCaP. Similarly, confocal microscopy further verified that the SCML2 immunoreactivity is higher in C4-2 than in LNCaP cells (Figures S3A and S3B). Our quantitative PCR consistently showed that SCML2 transcripts correlated with SCML2 protein levels (Figure S3C).

Notably, LNCaP and C4-2 cells with AR-full length (AR-FL) showed much higher levels of SCML2 reactivity than the 22Rv1, which mainly harbors a short AR-v7 form that lacks the ligand binding domain (Figure 2A). Consistent with this notion, androgen exposure enhanced the SCML2 nuclear accumulation in LNCaP compared to the vehicle control (Figure 2C, Lane 4 vs. Lane 2). On the other hand, a potent, direct AR inhibitor ENZ reduced the SCML2 nuclear intensity (Figure 2C, Lane 6 vs. Lane 4), coinciding with a slight increase in SCML2 protein in the cytoplasm (Figure 2C, Lane 5 vs. Lane 3 vs. Lane 1). Similarly, androgen exposure increased the SCML2 nuclear reactivity in C4-2 cells

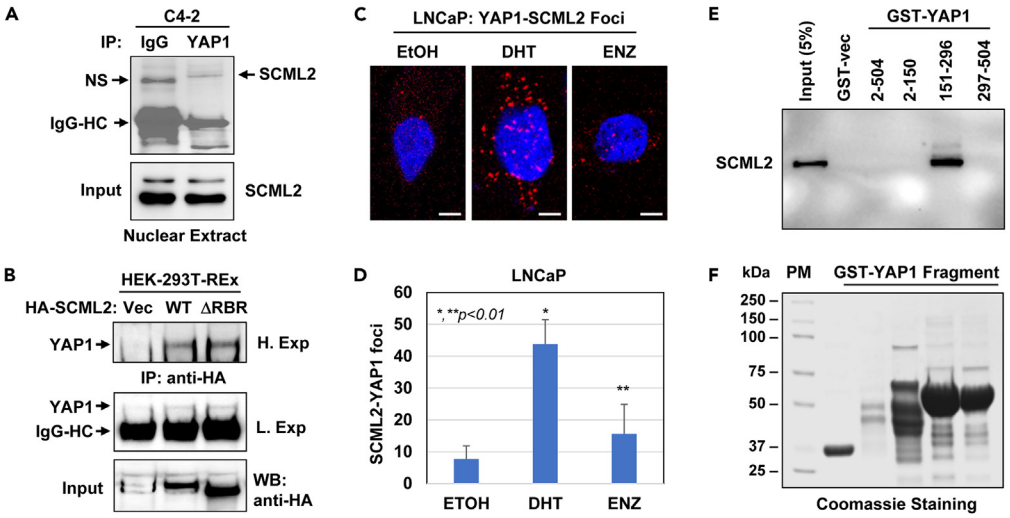

Figure 3. Protein complex formation between SCML2 and YAP1 under varying conditions

(A) Native SCML2 is co-immunoprecipitated with YAP1 protein in C4-2 cells grown in serum-fed conditions.

(B) Co-IP of YAP1 with HA-Mock Vector (Vec), HA-SCML2-WT, or HA-SCML2-ΔRBR protein ectopically expressed in HEK-293 cells. ΔRBR denotes the deletion of RNA binding region. H: High exposure, L: Low exposure.

(C) Proximity ligation assay (PLA) showing protein-protein interaction (the foci in red) between SCML2 and YAP1 in LNCaP cells, as visualized by confocal microscopy. The interaction of SMCL2 with YAP1 was assessed using SCML2 (G1) antibody. The size bar: 10 μm.

(D) The graph shows the quantification of the foci. Cells were treated with EtOH, DHT (10 nM), and ENZ (20 μM) in DCC serum-fed conditions for 16h.

(E and F) GST pulldown assay with the recombinant GST-YAP1 peptide fragment. Nuclear extract isolated from LNCaP cells under steady-state growth conditions was used as a source of SCML2 protein in GST pulldown assay. PM: protein marker. Data are represented as mean ± SEM of at least three independent experiments.

compared to the vehicle treatment (Figure 2C, Lane 4 vs. Lane 2). However, unlike LNCaP cells, ENZ slightly enhanced the nuclear reactivity of SCML2 in C4-2 cells (Figure 2D, Lane 6 vs. Lane 4). This observation coincided with immunofluorescence imaging regarding the subcellular distributions of SCML2 in LNCaP and C4-2 cells under the same treatment conditions (Figures 2E and 2F, respectively).

SCML2 physically interacts with YAP1

To verify the proteomics data and demonstrate whether YAP1 and SCML2 physically interact with each other, we conducted a series of protein-protein interaction assays under varying conditions. First, coimmunoprecipitation (co-IP) combined with western blot (WB) showed that native SCML2 and YAP1 formed protein complexes (Figure 3A). Similarly, co-IP/WB also showed that ectopic SCML2 interacted with endogenous YAP1 in HEK-293T-REx cells engineered to express stable vector, SCML2-WT or SCML2-ΔRBR (RNA-binding region-deleted SCML2) (Figure 3B). The results also indicated that protein-protein interaction between SCML2 and YAP1 occurred independently of RNA and RBR of SCML2 because the deletion of RBR did not alter the interaction of SCML2 with YAP1.

Next, we conducted a proximity ligation assay (PLA) to determine whether androgen regulates protein-protein interaction between YAP1 and SCML2. The PLA demonstrated that compared to the control, DHT exposure enhanced the YAP1 and SCML2 interaction while ENZ attenuated it (Figures 3C, 3D, and S4), indicating that the YAP1 and SCML2 interaction is specific and an androgen-regulated event. Finally, to further verify the physical interaction between YAP1 and SCML2 and to identify the YAP1 protein domains that mediate interaction with SCML2, we conducted a GST pulldown assay using the recombinant YAP1 truncation mutants fused to GST peptides. GST pulldown showed that SCML2 interacted with the YAP1 fragment (residue 151–296) that harbors the WW/SH3 domain. Unfortunately, we could not express the full-length YAP1 as a GST fusion protein, consistent with our previous observation.[34]

SCML2 and YAP1 are functionally antagonistic

To determine the functional consequence of protein-protein interaction between SCML2 and YAP1, we assessed SCML2 and YAP1 protein expression in cells with or without SCML2 knockdown by siRNA. Silencing SCML2 increased YAP1 protein levels 2.8-fold relative to the scramble siRNA control (Figure 4A). The effects of SCML2 on YAP1 are biologically functional because SCML2 depletion enhanced the YAP1-mediated TEAD-responsive promoter-reporter gene activation about three-fold compared to the scramble siRNA control (Figure 4B). The observation is specific because silencing YAP1 attenuated the promoter-directed reporter gene activation by TEAD (Figure 4B), given that TEAD requires YAP1 to activate its target gene transcription.[40]

Furthermore, the STK4-encoded MST1 kinase phosphorylates the Ser127 (S127) residue and inactivates YAP1 through cytoplasmic sequestration and proteasomal degradation.[33,34,41] Thus, we suggest that SCML2 cooperate with STK4/MST1 to antagonize YAP1. Indeed, silencing

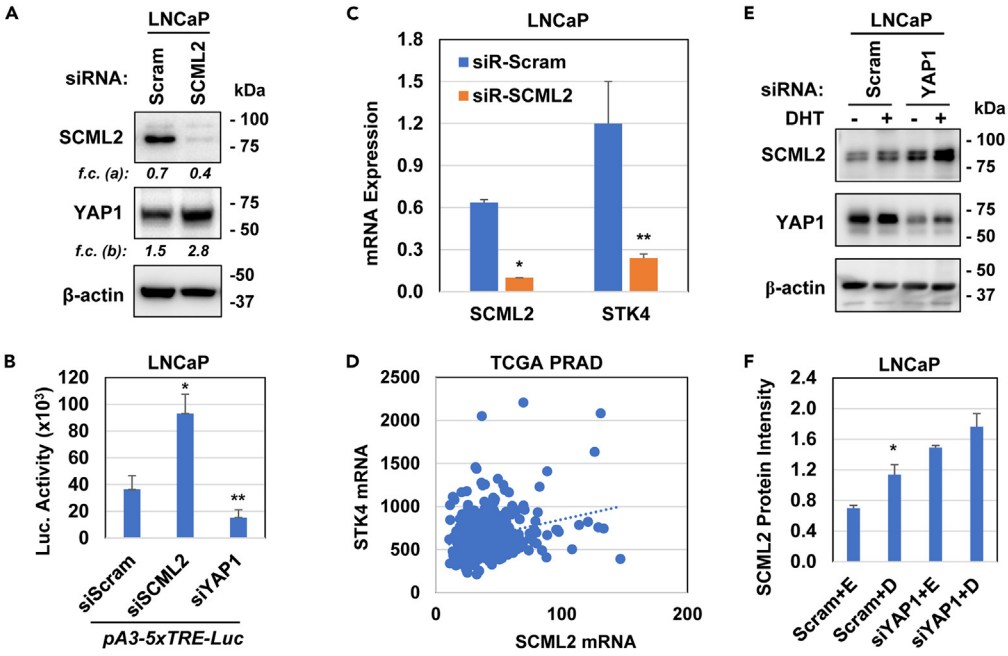

Figure 4. YAP1 and SCML2 activity inversely correlate

(A) Immunoblots of YAP1 and SCML2 protein with or without SCML2 knockdown conditions. SCML2 blot was generated with the SCML2 (G1) antibody.

(B) YAP1-mediated promoter-luciferase (Luc) reporter gene activity with or without SCML2 or YAP1 knockdown conditions, *, **p > 0.01.

(C) Quantitative PCR analysis of STK4-encoded MST1 transcripts in LNCaP cells with or without SCML2 knockdown by siRNA, *p > 0.001.

(D) SCML2 and STK4 transcripts positively correlate in human prostate tumor tissues, Pearson correlation: 0.29, p = 2.46e-11.

(E) Immunoblots of YAP1 and SCML2 in LNCaP cells after treatment with vehicle (–) or DHT with (+) and transiently transfected with the scramble (scram) or YAP1 siRNA under 5% DCC serum-fed growth condition. Beta-actin blots were used as a loading control.

(F) The graph shows the quantification of the SCML2 blot in panel E, *p > 0.01. Data are represented as mean ± SEM of three independent experiments.

SCML2 reduced STK4 transcripts compared to the siRNA control (Figure 4C). This observation could be physiological because the computational analysis of The Cancer Genome Atlas (TCGA) prostate adenocarcinoma (PRAD) dataset, accessible via the cBioPortal (RRID: SCR_014555),[42] showed that STK4 and SCML2 transcripts positively correlated (Pearson: 0.29; p = 2.46e-11) (Figure 4D).

To determine whether YAP1 modulates SCML2 activity, we assessed SCML2 protein levels in LNCaP cells with or without YAP1 knockdown and androgen treatment conditions. Silencing YAP1 enhanced SCML2 protein levels significantly compared to the scramble siRNA during EtOH (vehicle) treatment, and androgen further elevated SCML2 protein levels relative to the vehicle control (Figure 4E). Altogether, these observations indicate functional antagonisms exist between YAP1 and SCML2.

SCML2 differentially regulates cell growth

Our earlier work showed that YAP1 promoted cell growth and cell survival because genetic silencing of YAP reduced cell growth in 2D and 3D cultures *in vitro* and tumor growth in mice.[34] In addition, Figure 4 indicates that SCML2 antagonizes YAP1 activity or vice versa. Also, androgen differentially regulates SCML2 activity in AD LNCaP and AI C4-2 cells. Consequently, we propose that SCML2 distinctly governs the growth of LNCaP and C4-2 cells. To test this idea, we evaluated the growth of LNCaP and C4-2 cells with or without SCML2 depletion and EtOH (vehicle), DHT, and ENZ treatments. Notably, silencing SCML2 significantly increased the growth of LNCaP by androgen. Ironically, ENZ failed to inhibit the growth in SCML2 knockdown conditions (Figures 5A, 5B, S5A, and S5B). Unlike LNCaP cells, however, silencing SCML2 modestly but significantly reduced C4-2 cell growth after DHT or ENZ treatment (Figures 5C, 5D, S5C, and S5D). Moreover, we also tested the effects of SCML2 knockdown on another AR-positive C4-B cell line, a bone-metastatic subline of C4-2.[35] The pattern of the growth by SCML2 knockdown in response to EtOH, DHT, and ENZ treatment is similar to that of C4-2 cells (not shown). Furthermore, our PLA showed a weak protein-protein interaction between SCML2 and YAP1, even in the presence of androgen (Figure S6), indicating that the mechanism regulating SCML2 and YAP1 protein-protein interaction in LNCaP and C4-2 cells are different.

SCML2 and YAP1 distinctly modify histones

A growing body of research suggests that SCML2 mainly exerts its cellular biology through epigenetic mechanisms. For example, SCML2 modulates tri-methylation of histone 3 on lysine 27 (H3K27me3)[13,23] and monoubiquitylation of H2A at lysine 119 (H2AK119Ub).[11,43] Both histone modifications are critical for gene regulation, particularly during development.[11–13,23] Therefore, to gain further mechanistic insights into

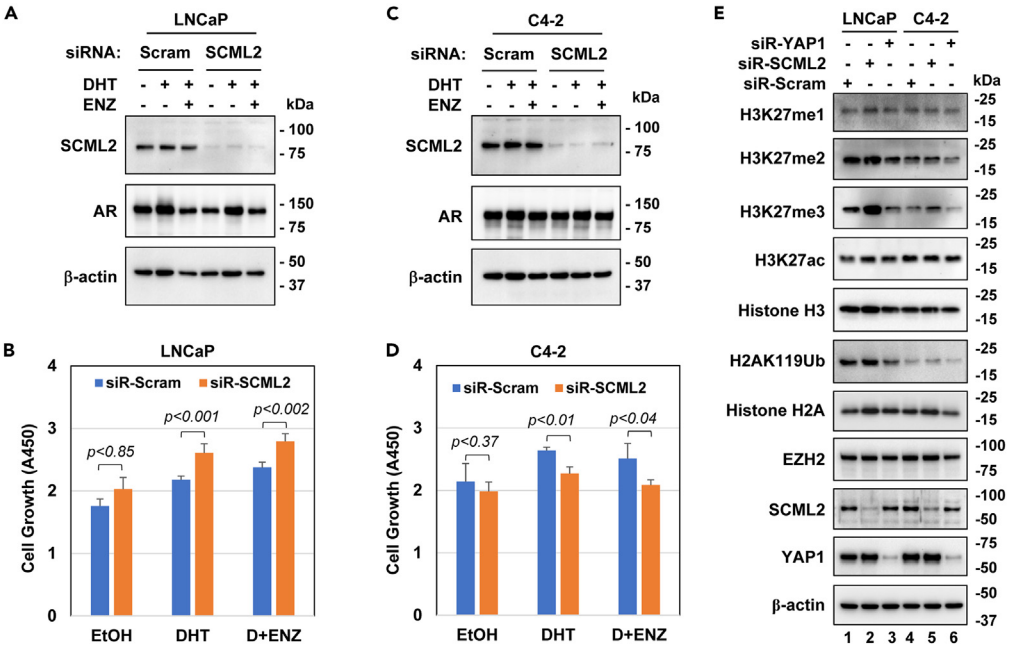

Figure 5. SCML2 regulates cell growth in a context-dependent manner

(A–D) Analysis of SCML2 in LNCaP and C4-2 cells under Scrambled (control) siRNA (siR-Scram) or SCML2 siRNA knockdown, followed by treatment with EtOH (vehicle), DHT (D: 10 nM), or ENZ (20 μM) in DCC serum-fed growth conditions. The SCML2 blot was generated using the SCML2 (G1) antibody. AR blots were included in these experiments to monitor the responsiveness of androgen hormone signaling. Beta-actin blots were included as a loading control. Cell growth was assessed by CCK-8 assay at 48h post-treatment in DCC serum-fed conditions. Data are three independent experiments in triplicates each.

(E) Analysis of the gene regulatory histone marks in LNCaP and C4-2 cells with or without SCML2 and YAP1 knockdown conditions. Data are represented as mean ± SEM of three independent experiments.

the interaction between SCML2 and YAP1, we analyzed the immunoreactivity of H3K27me3 and H2AK119Ub histone marks in LNCaP and C4-2 cells with or without SCML2 or YAP1 knockdown (Figure 5E). We also evaluated the immunoreactivity of H3K27me1, H3K27me2, and a gene-activating histone mark H3K27ac (acetylation) as controls under the same experimental conditions (Figure 5E).

The results showed that the reactivity of H3K27me3 and H3K27me2 was much lower in C4-2 than in LNCaP, although both cell lines expressed similar levels of H3K27me1. SCML2 knockdown markedly increased the H3K27me3 reactivity compared to the H3K27me1 and H3K27me2. Nevertheless, YAP1 knockdown reduced the immunoreactivity of H3K27me3 compared to the control siRNA in LNCaP and C4-2 cells. These observations appear specific because depletion of SCML2 or YAP1 did not change the levels of H3K27ac, beta-actin (a housekeeping protein), and EZH2, an enzyme that catalyzes H3K27me3. The data also showed that the reactivity of H2AK119Ub is markedly lower in C4-2 than in LNCaP cells. Finally, while silencing SCML2 increased H2AK119Ub levels, YAP1 knockdown had the opposite effect. These observations demonstrate that SCML2 and YAP1 inversely regulate H3K27me3 and H2AK119Ub activity, at least in LNCaP and C4-2 cells.

SCML2 and YAP1 target genes overlap

To gain new insights into the SCML2 and YAP1 interaction, we analyzed the existing data of the protein-coding, SCML2 target genes (n = 726) from the genetically modified HEK-293T-REs cell line[16] and the protein-coding, YAP1 target genes (n = 3297) from the genetically modified CAL-51 primary breast cell line.[44] The analysis identified 226 genes (~31%) as overlapping targets of SCML2 and YAP1 (Figure 6A, Table S3). The GO analysis by functional annotation clustering demonstrated that SCML2 and YAP1 overlapping targets are associated with diverse biological processes or pathways, including cell communication, differentiation, protein binding, and gene expression (Figure 6B). In addition, we manually inspected the 226 overlapping genes and identified 20 relatively well-studied proteins. Our literature search in PubMed showed the 20 genes or proteins directly or indirectly interact with YAP1 (Figure S6), but their interactions with SCML2 are unknown.

Surprisingly, EPHA3 is one of the overlapping YAP1 and SCML2 target genes. We have recently reported that the YAP1/TEAD1 transcriptionally regulates EPHA3 expression downstream of the Hippo/STK4 pathway.[40] Notably, YAP1 and SCML2 could control the expression of EMT transcription factor ZEB1, and our ongoing study suggests that EPHA3 regulates ZEB1 expression in C4-2 cells (not shown). In addition, both YAP1 and SCML2 could target SCML1, a paralog of SCML2, although our proteomics did not identify SCML1 as an interacting partner of the YAP1 protein complexes. Moreover, our protein network analysis showed that these 20 genes are associated with each other by >97% through co-expression (Figure 6C).

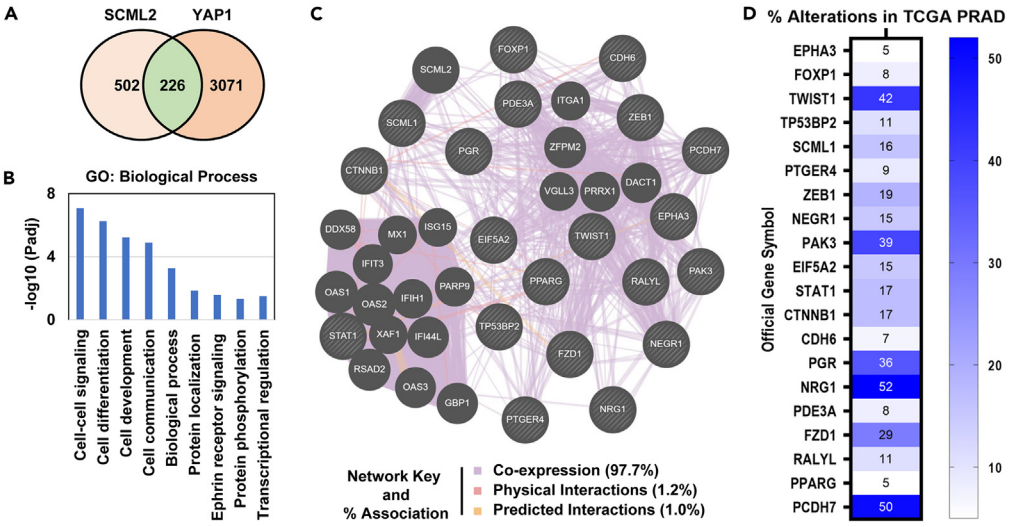

Figure 6. A significant number of the SCML2 target genes overlap with the YAP1 targets

(A) Venn diagram shows the unique and overlapping targets of SCML2 and YAP1.

(B) The 226 overlapping targets of SCML2 and YAP1 are associated with diverse biological processes.

(C) The protein network of the 20 gene set.

(D) Percent alteration of the 20 genes in prostate adenocarcinoma (PRAD) dataset in The Cancer Genome Atlas (TCGA).

To evaluate the physiological or clinical significance of the 20 gene set in the context of cancer, we computed these 20 genes against the TCGA PRAD dataset. Expressions of these genes were altered in prostate tumor tissues, ranging from 5% to 52%, mostly downregulation (Figure 6D, Table S4). Likewise, our computational analysis showed that the remaining SCML2 and YAP1 overlapping genes (n = 206) were also altered to varying percentages in prostate tumor samples, and the alterations were similar to the data presented in Figure 6D. These observations further solidify the molecular and functional connection between YAP1 and SCML2. In addition, the distinct and overlapping genes regulated by YAP1 and SCML2 may provide critical insights into the biology of differential cell growth by SCML2 under changing cell environments. Moreover, SCML2 and YAP1 cooperate to regulate the molecular processes of cell growth, cell survival, and tumorigenesis.

DISCUSSION

The current study demonstrates novel biochemical and functional interactions between the YAP1 and epigenetic regulatory protein SCML2 in human cells. We have provided compelling data to support the conclusion. First, our MS-based proteomics analysis combined with co-IP identified SCML2 as a YAP1 interacting protein. Second, our immunological assays showed that the AR-positive cell lines express SCML2 and that androgen hormone signaling regulates the interaction of SCML2 with YAP1. Third, the GST pulldown assay showed that the WW/SH3 domain of YAP1 mediated protein-protein interaction with SCML2. Fourth, our gene silencing data showed that YAP1 and SCML2 are functionally antagonistic. Finally, SCML2 might function as a growth suppressor in androgen-sensitive LNCaP cells while functioning as a survival factor in androgen-insensitive C4-2 cells, likely due to discordant YAP1 and SCML2 interaction, epigenetic alterations, and differential gene expression. Thus, our findings suggest that mutual interactions between YAP1 and SCML2 play critical roles in cellular biology and human diseases such as cancer.

Our proteomics analyses identified several RBPs associated with the YAP1 protein complexes. Emerging literature indicates that proteins regulating RNA biogenesis and modifications also interact with and modulate the YAP1 localization and functions.[45,46] Similarly, RBPs could regulate Drosophila protein *Yki*, a YAP1 ortholog.[47] Likewise, Howell et al.[48] showed biochemical and functional interactions between an RBP HNRNPU and YAP1. Our LC-MS/MS proteomics identified HNRNPU as one of the YAP1 interacting proteins. In addition, a study by Bonasio et al.[16] showed that SCML2 could interact with RNA via its RNA-binding region. Herein, we identified SCML2 as a YAP1-associated protein and demonstrated that native SCML2 protein biochemically and functionally interacts with endogenous YAP1. Therefore, our observation, consistent with the literature, indicates that YAP1 interacts with RBPs, which we have been exploring this possibility.

The AR is a member of the nuclear receptor family, and as far as we know, it is the sole mediator of androgens (testosterone and 5-hydroxytestosterone) actions. Here, we have identified SCML2 from the AR-positive cell models. Our data showed that androgen exposure induced the interaction of SCML2 with YAP1, particularly in the AD cell line. In addition, a published study demonstrated that androgen promoted protein-protein interaction between YAP1 and AR.[34] In that study, AR interacted with the YAP1 protein regions that harbor the WW and SH3 domains.[34] Herein, we also identified the same YAP1 region that mediated the interaction with SCML2, suggesting the possibility that AR is part of the YAP1/SCML2 protein complex and mediates protein-protein interaction between YAP1 and SCML2. Thus, future studies are warranted to dissect a detailed mechanism of YAP1 and SCML2 interactions and to demonstrate whether YAP1 and SCML2 cooperate to contribute to cellular activities in disease or non-disease models, particularly in the context of androgen/AR signaling. Herein, we did not

attempt to assess the interaction of SCML2 with WWTR1/TAZ, a close paralog of YAP1, because the LNCaP and C4-2 cell lines do not express WWTR1/TAZ.[33,34]

Moreover, our protein network analysis has uncovered no direct interaction between SCML2 and YAP1 until now; however, other factors may directly or indirectly facilitate the YAP1 and SCML2 interaction. For example, RNF4 (ring finger protein 4, an SUMO-targeted ubiquitin E3 ligase) might mediate a physical interaction between SCML2 and YAP1. Similarly, the KDM1A-encoded LSD1 (a lysine-specific histone demethylase 1A) and the YWHAZ-encoded 14-3-3ζ (tyrosine 3-monooxygenase/tryptophan 5-monooxygenase activation protein zeta) may also facilitate the association of SCML2 with YAP1. Our proteomics identified 14-3-3ζ as a YAP1 interacting protein. The 14-3-3 family members, like 14-3-3ζ, are known to bind and regulate YAP1, such as in hypoxic glycolysis.[49,50] Likewise, the LSD1/KDM1A and the AR pioneering factor FOXA1 were shown to interact with and regulate AR activity.[51] Also, BAG1 (BCL2-associated athanogene 1) is part of the YAP1 and SCML2 network, and BAG1 could provide cell survival[52] and might have important roles in determining cell fate by SCML2 and YAP1. Moreover, the transcription factor TEAD1 is a critical mediator of YAP1.[40] Notably, TEAD1 genetically interacts with YWHAZ, BAG1, and KDM1A, indicating that SCML2 is part of the YAP1/TEAD protein network and a critical epigenetic regulator of the YAP1/TEAD-dependent gene transcription.

Furthermore, our data showed that SCML2 could regulate cell growth and survival in a divergent mechanism. Evidence suggests that crosstalk between the cell-cycle machinery and the cellular memory of the Polycomb system is critical for regulating cell growth.[53] A published study showed that the CDK/CYCLIN kinase interacted with and phosphorylated SCML2 in a cell cycle-dependent manner.[53] In that study, the author showed that the interaction of SCML2 with cell-cycle regulators p21 and p27 further enhanced the growth-suppressive effects of p21 and p27. In the current research, our data showed that SCML2 might suppress cell growth by counter-interacting with YAP1, possibly in a cell or tissue-specific manner because silencing SCML2 increased LNCaP cell growth by androgens while reducing the growth-suppressive effects of anti-androgen, ENZ. However, silencing SCML2 minimized C4-2 growth while enhancing the cell-killing efficacy of ENZ. In addition, studies from our laboratory and others showed that YAP1 promotes cell proliferation and survival.[34,54] Here, we demonstrated that silencing SCML2 enhanced the induction of YAP1-dependent promoter activation, which coincided with reduced STK4 expression, a potent inhibitor of YAP1. This observation is consistent with our published studies that altered STK4/MST1 signaling plays essential roles in cell growth and survival.[55,56] As such, SCML2 may control the Hippo/STK4 activity to modulate YAP1 in addition to the protein-protein interaction. Nevertheless, future studies warrant uncovering the mechanism by which SCML2 regulates STK4 that may be critical for the negative regulation of YAP1 activity by SCML2.

Finally, our earlier work showed that disruption of YAP1 activity reduced cell growth *ex vivo* and *in vivo*.[34] The present study showed that YAP1 and SCML2 biochemically and functionally interact, and their interaction might be crucial for controlling cell growth. Also, our study indicates that dysregulated SCML2 activity plays a significant role in prostate tumor biology, given that SCML2 expression is increased in the AI tumor cell lines, in which SCML2 weakly interacted with YAP1. Thus, we suggest that the relative YAP1 and SCML2 activity and the degree of their interaction could determine the growth behaviors of the cell. In addition, our study indicates that SCML2 and YAP1 cooperate to regulate prostate tumor biology because many SCML2 and YAP1 target genes overlap (Figure 6). Therefore, further studies are needed to assess the significance of SCML2 in prostate tumor progression, particularly in the context of YAP1 and/or AR, which could identify the YAP1-SCML2-AR axis as a promising cancer drug target.

Limitations of the study

This study is the first to show that YAP1 and SCML2 biochemically and functionally interact with each other in the cell. However, we recognize that a limited mechanistic explanation supports this conclusion. First, our study did not provide a direct mechanism underlying how SCML2 regulates cell growth in response to androgen signaling, and whether that occurs in a YAP1-dependent or YAP1-independent manner remains to be discovered. Second, our study did not examine whether SCML2 cooperates with other members of the PRC1 or PRC2 to regulate YAP1 activity, which occurred in a TEAD-dependent or independent manner. Despite these limitations, our study indicates that altered SCML2 activity appears essential for androgen-dependent and androgen-independent cell growth and survival. In addition, our study uncovered that, unlike the SCML2 knockdown, the YAP1 knockdown reduced the gene-suppressive H3K27me3 and H2AK119Ub histone marks, implicating a functional yet opposing association between YAP1 and SCML2. The opposing histone modifications may lead to distinct and overlapping gene expression by SCML2 and YAP1, likely in connection with the PRC1/2.[27] Thus, these novel findings warrant future studies to define the molecular basis and the physiological significance of SCML2 and YAP1 interaction regulating histone modifications and gene expression. These studies may constitute the SCML2-YAP1 axis as an essential pathway that plays a crucial role in cellular physiology and human diseases such as cancer development and progression, particularly downstream of steroid hormones like androgens.

STAR★METHODS

Detailed methods are provided in the online version of this paper and include the following:

- KEY RESOURCES TABLE
- RESOURCE AVAILABILITY
  - Lead contact
  - Materials availability
  - Data and code availability
- EXPERIMENTAL MODEL AND STUDY PARTICIPANT DETAILS

SUPPLEMENTAL INFORMATION

Supplemental information can be found online at https://doi.org/10.1016/j.isci.2023.107964.

ACKNOWLEDGMENTS

We thank Drs. Roberto Bonasio and Emilio Lecona for providing the SCML2 expressing HEK-293T cell line and SCML2 expression plasmids. Also, we thank Dr. Bonasio for critically reviewing the manuscript and providing helpful comments. National Science Foundation–Division of Molecular and Cellular Biosciences grant #1832022 (to BC), National Institutes of Health/NIMHD grant #2U54MD007590-32 (to the Center for Cancer Research and Therapeutic Program, Clark Atlanta University), and the NIH/NIGMS/RISE Program Grant #5R25GM060414 (to the Departments of Chemistry and Biological Sciences at Clark Atlanta University) support this work.

AUTHOR CONTRIBUTIONS

B.C. conceptualized the idea, provided resources, and acquired funding; A.M.B., A.M.D., M.M.A-M., and B.C. designed and executed the experiments, curated, analyzed, validated the data, and prepared Figures and Tables; J.Z., Q.Z., and G.W. conducted LC-MS/MS proteomics analysis; K.K. provided technical support; B.C., A.M.B., A.M.D., and M.M.A-M. wrote and revised the manuscript.

DECLARATION OF INTERESTS

The authors declare no conflict of interest.

INCLUSION AND DIVERSITY

One or more of the authors of this paper self-identifies as an underrepresented ethnic minority in their field of research or within their geographical location. One or more of the authors of this paper received support from a program designed to increase minority representation in their field of research.

Received: December 20, 2022
Revised: May 25, 2023
Accepted: September 15, 2023
Published: September 20, 2023

REFERENCES

1. Schwartz, Y.B., and Pirrotta, V. (2008). Polycomb complexes and epigenetic states. Curr. Opin. Cell Biol. *20*, 266–273. https://doi.org/10.1016/j.ceb.2008.03.002.
2. Kundu, S., Ji, F., Sunwoo, H., Jain, G., Lee, J.T., Sadreyev, R.I., Dekker, J., and Kingston, R.E. (2017). Polycomb Repressive Complex 1 Generates Discrete Compacted Domains that Change during Differentiation. Mol. Cell *65*, 432–446.e5. https://doi.org/10.1016/j.molcel.2017.01.009.
3. Levine, S.S., Weiss, A., Erdjument-Bromage, H., Shao, Z., Tempst, P., and Kingston, R.E. (2002). The core of the polycomb repressive complex is compositionally and functionally conserved in flies and humans. Mol. Cell Biol. *22*, 6070–6078. https://doi.org/10.1128/mcb.22.17.6070-6078.2002.
4. Blackledge, N.P., Farcas, A.M., Kondo, T., King, H.W., McGouran, J.F., Hanssen, L.L.P., Ito, S., Cooper, S., Kondo, K., Koseki, Y., et al. (2014). Variant PRC1 complex-dependent H2A ubiquitylation drives PRC2 recruitment and polycomb domain formation. Cell *157*, 1445–1459. https://doi.org/10.1016/j.cell.2014.05.004.
5. Bezsonova, I. (2014). Solution NMR structure of the DNA-binding domain from Scml2 (sex comb on midleg-like 2). J. Biol. Chem. *289*, 15739–15749. https://doi.org/10.1074/jbc.M113.524009.
6. Montini, E., Buchner, G., Spalluto, C., Andolfi, G., Caruso, A., den Dunnen, J.T., Trump, D., Rocchi, M., Ballabio, A., and Franco, B. (1999). Identification of SCML2, a second human gene homologous to the Drosophila sex comb on midleg (Scm): A new gene cluster on Xp22. Genomics *58*, 65–72. https://doi.org/10.1006/geno.1999.5755.
7. Meier, K., and Brehm, A. (2014). Chromatin regulation: how complex does it get?

Epigenetics *9*, 1485–1495. https://doi.org/10.4161/15592294.2014.971580.

8. Wang, L., Jahren, N., Miller, E.L., Ketel, C.S., Mallin, D.R., and Simon, J.A. (2010). Comparative analysis of chromatin binding by Sex Comb on Midleg (SCM) and other polycomb group repressors at a Drosophila Hox gene. Mol. Cell Biol. *30*, 2584–2593. https://doi.org/10.1128/mcb.01451-09.
9. Takada, Y., Isono, K.i., Shinga, J., Turner, J.M.A., Kitamura, H., Ohara, O., Watanabe, G., Singh, P.B., Kamijo, T., Jenuwein, T., et al. (2007). Mammalian Polycomb Scmh1 mediates exclusion of Polycomb complexes from the XY body in the pachytene spermatocytes. Development *134*, 579–590. https://doi.org/10.1242/dev.02747.
10. Bonasio, R., Lecona, E., and Reinberg, D. (2010). MBT domain proteins in development and disease. Semin. Cell Dev. Biol. *21*, 221–230. https://doi.org/10.1016/j.semcdb.2009.09.010.
11. Maezawa, S., Hasegawa, K., Alavattam, K.G., Funakoshi, M., Sato, T., Barski, A., and Namekawa, S.H. (2018). SCML2 promotes heterochromatin organization in late spermatogenesis. J. Cell Sci. *131*, jcs217125. https://doi.org/10.1242/jcs.217125.
12. Hasegawa, K., Sin, H.S., Maezawa, S., Broering, T.J., Kartashov, A.V., Alavattam, K.G., Ichijima, Y., Zhang, F., Bacon, W.C., Greis, K.D., et al. (2015). SCML2 establishes the male germline epigenome through regulation of histone H2A ubiquitination. Dev. Cell *32*, 574–588. https://doi.org/10.1016/j.devcel.2015.01.014.
13. Maezawa, S., Hasegawa, K., Yukawa, M., Kubo, N., Sakashita, A., Alavattam, K.G., Sin, H.S., Kartashov, A.V., Sasaki, H., Barski, A., and Namekawa, S.H. (2018). Polycomb protein SCML2 facilitates H3K27me3 to establish bivalent domains in the male germline. Proc. Natl. Acad. Sci. USA *115*, 4957–4962. https://doi.org/10.1073/pnas.1804512115.
14. Santiveri, C.M., Lechtenberg, B.C., Allen, M.D., Sathyamurthy, A., Jaulent, A.M., Freund, S.M.V., and Bycroft, M. (2008). The malignant brain tumor repeats of human SCML2 bind to peptides containing monomethylated lysine. J. Mol. Biol. *382*, 1107–1112. https://doi.org/10.1016/j.jmb.2008.07.081.
15. Sathyamurthy, A., Allen, M.D., Murzin, A.G., and Bycroft, M. (2003). Crystal structure of the malignant brain tumor (MBT) repeats in Sex Comb on Midleg-like 2 (SCML2). J. Biol. Chem. *278*, 46968–46973. https://doi.org/10.1074/jbc.M306469200.
16. Bonasio, R., Lecona, E., Narendra, V., Voigt, P., Parisi, F., Kluger, Y., and Reinberg, D. (2014). Interactions with RNA direct the Polycomb group protein SCML2 to chromatin where it represses target genes. Elife *3*, e02637. https://doi.org/10.7554/eLife.02637.
17. Dobrinić, P., Szczurek, A.T., and Klose, R.J. (2021). PRC1 drives Polycomb-mediated gene repression by controlling transcription initiation and burst frequency. Nat. Struct. Mol. Biol. *28*, 811–824. https://doi.org/10.1038/s41594-021-00661-y.
18. Blackledge, N.P., and Klose, R.J. (2021). The molecular principles of gene regulation by Polycomb repressive complexes. Nat. Rev. Mol. Cell Biol. *22*, 815–833. https://doi.org/10.1038/s41580-021-00398-y.
19. Tavares, L., Dimitrova, E., Oxley, D., Webster, J., Poot, R., Demmers, J., Bezstarosti, K., Taylor, S., Ura, H., Koide, H., et al. (2012). RYBP-PRC1 complexes mediate H2A ubiquitylation at polycomb target sites independently of PRC2 and H3K27me3. Cell *148*, 664–678. https://doi.org/10.1016/j.cell.2011.12.029.
20. Menon, D.U., Shibata, Y., Mu, W., and Magnuson, T. (2019). Mammalian SWI/SNF collaborates with a polycomb-associated protein to regulate male germline transcription in the mouse. Development *146*, dev174094. https://doi.org/10.1242/dev.174094.
21. Wang, H., Wang, L., Erdjument-Bromage, H., Vidal, M., Tempst, P., Jones, R.S., and Zhang, Y. (2004). Role of histone H2A ubiquitination in Polycomb silencing. Nature *431*, 873–878. https://doi.org/10.1038/nature02985.
22. de Napoles, M., Mermoud, J.E., Wakao, R., Tang, Y.A., Endoh, M., Appanah, R., Nesterova, T.B., Silva, J., Otte, A.P., Vidal, M., et al. (2004). Polycomb group proteins Ring1A/B link ubiquitylation of histone H2A to heritable gene silencing and X inactivation. Dev. Cell *7*, 663–676. https://doi.org/10.1016/j.devcel.2004.10.005.
23. Adams, S.R., Maezawa, S., Alavattam, K.G., Abe, H., Sakashita, A., Shroder, M., Broering, T.J., Sroga Rios, J., Thomas, M.A., Lin, X., et al. (2018). RNF8 and SCML2 cooperate to regulate ubiquitination and H3K27 acetylation for escape gene activation on the sex chromosomes. PLoS Genet. *14*, e1007233. https://doi.org/10.1371/journal.pgen.1007233.
24. Luo, M., Zhou, J., Leu, N.A., Abreu, C.M., Wang, J., Anguera, M.C., de Rooij, D.G., Jasin, M., and Wang, P.J. (2015). Polycomb protein SCML2 associates with USP7 and counteracts histone H2A ubiquitination in the XY chromatin during male meiosis. PLoS Genet. *11*, e1004954. https://doi.org/10.1371/journal.pgen.1004954.
25. Zanconato, F., Forcato, M., Battilana, G., Azzolin, L., Quaranta, E., Bodega, B., Rosato, A., Bicciato, S., Cordenonsi, M., and Piccolo, S. (2015). Genome-wide association between YAP/TAZ/TEAD and AP-1 at enhancers drives oncogenic growth. Nat. Cell Biol. *17*, 1218–1227. https://doi.org/10.1038/ncb3216.
26. Lo Sardo, F., Pulito, C., Sacconi, A., Korita, E., Sudol, M., Strano, S., and Blandino, G. (2021). YAP/TAZ and EZH2 synergize to impair tumor suppressor activity of TGFBR2 in non-small cell lung cancer. Cancer Lett. *500*, 51–63. https://doi.org/10.1016/j.canlet.2020.11.037.
27. Hoxha, S., Shepard, A., Troutman, S., Diao, H., Doherty, J.R., Janiszewska, M., Witwicki, R.M., Pipkin, M.E., Ja, W.W., Kareta, M.S., and Kissil, J.L. (2020). YAP-Mediated Recruitment of YY1 and EZH2 Represses Transcription of Key Cell-Cycle Regulators. Cancer Res. *80*, 2512–2522. https://doi.org/10.1158/0008-5472.Can-19-2415.
28. Hillmer, R.E., and Link, B.A. (2019). The Roles of Hippo Signaling Transducers Yap and Taz in Chromatin Remodeling. Cells *8*. https://doi.org/10.3390/cells8050502.
29. Chang, L., Azzolin, L., Di Biagio, D., Zanconato, F., Battilana, G., Lucon Xiccato, R., Aragona, M., Giulitti, S., Panciera, T., Gandin, A., et al. (2018). The SWI/SNF complex is a mechanoregulated inhibitor of YAP and TAZ. Nature *563*, 265–269. https://doi.org/10.1038/s41586-018-0658-1.
30. Kim, M., Kim, T., Johnson, R.L., and Lim, D.S. (2015). Transcriptional co-repressor function of the hippo pathway transducers YAP and TAZ. Cell Rep. *11*, 270–282. https://doi.org/10.1016/j.celrep.2015.03.015.
31. Ma, S., Meng, Z., Chen, R., and Guan, K.-L. (2019). The Hippo Pathway: Biology and Pathophysiology. Annu. Rev. Biochem. *88*, 577–604. https://doi.org/10.1146/annurev-biochem-013118-111829.
32. Pavel, M., Renna, M., Park, S.J., Menzies, F.M., Ricketts, T., Füllgrabe, J., Ashkenazi, A., Frake, R.A., Lombarte, A.C., Bento, C.F., et al. (2018). Contact inhibition controls cell survival and proliferation via YAP/TAZ-autophagy axis. Nat. Commun. *9*, 2961. https://doi.org/10.1038/s41467-018-05388-x.
33. Cinar, B., Al-Mathkour, M.M., Khan, S.A., and Moreno, C.S. (2020). Androgen attenuates the inactivating phospho-Ser-127 modification of yes-associated protein 1 (YAP1) and promotes YAP1 nuclear abundance and activity. J. Biol. Chem. *295*, 8550–8559. https://doi.org/10.1074/jbc.RA120.013794.
34. Kuser-Abali, G., Alptekin, A., Lewis, M., Garraway, I.P., and Cinar, B. (2015). YAP1 and AR interactions contribute to the switch from androgen-dependent to castration-resistant growth in prostate cancer. Nat. Commun. *6*, 8126. https://doi.org/10.1038/ncomms9126.
35. Thalmann, G.N., Anezinis, P.E., Chang, S.M., Zhau, H.E., Kim, E.E., Hopwood, V.L., Pathak, S., von Eschenbach, A.C., and Chung, L.W. (1994). Androgen-independent cancer progression and bone metastasis in the LNCaP model of human prostate cancer. Cancer Res. *54*, 2577–2581.
36. Zanconato, F., Cordenonsi, M., and Piccolo, S. (2016). YAP/TAZ at the Roots of Cancer. Cancer Cell *29*, 783–803. https://doi.org/10.1016/j.ccell.2016.05.005.
37. Zanconato, F., Cordenonsi, M., and Piccolo, S. (2019). YAP and TAZ: a signalling hub of the tumour microenvironment. Nat. Rev. Cancer *19*, 454–464. https://doi.org/10.1038/s41568-019-0168-y.
38. Luo, J., and Li, P. (2022). Context-dependent transcriptional regulations of YAP/TAZ in stem cell and differentiation. Stem Cell Res. Ther. *13*, 10. https://doi.org/10.1186/s13287-021-02686-y.
39. Szulzewsky, F., Holland, E.C., and Vasioukhin, V. (2021). YAP1 and its fusion proteins in cancer initiation, progression and therapeutic resistance. Dev. Biol. *475*, 205–221. https://doi.org/10.1016/j.ydbio.2020.12.018.
40. Al-Mathkour, M.M., Dwead, A.M., Alp, E., Boston, A.M., and Cinar, B. (2022). The Hippo effector YAP1/TEAD1 regulates EPHA3 expression to control cell contact and motility. Sci. Rep. *12*, 3840. https://doi.org/10.1038/s41598-022-07790-4.
41. Avruch, J., Zhou, D., Fitamant, J., and Bardeesy, N. (2011). Mst1/2 signalling to Yap: gatekeeper for liver size and tumour development. Br. J. Cancer *104*, 24–32. https://doi.org/10.1038/sj.bjc.6606011.
42. Cerami, E., Gao, J., Dogrusoz, U., Gross, B.E., Sumer, S.O., Aksoy, B.A., Jacobsen, A., Byrne, C.J., Heuer, M.L., Larsson, E., et al. (2012). The cBio cancer genomics portal: an open platform for exploring multidimensional cancer genomics data. Cancer Discov. *2*, 401–404. https://doi.org/10.1158/2159-8290.Cd-12-0095.
43. Eskeland, R., Leeb, M., Grimes, G.R., Kress, C., Boyle, S., Sproul, D., Gilbert, N., Fan, Y., Skoultchi, A.I., Wutz, A., and Bickmore, W.A. (2010). Ring1B compacts chromatin structure and represses gene expression independent of histone ubiquitination. Mol. Cell *38*, 452–464. https://doi.org/10.1016/j.molcel.2010.02.032.

44. Nardone, G., Oliver-De La Cruz, J., Vrbsky, J., Martini, C., Pribyl, J., Skládal, P., Pešl, M., Caluori, G., Pagliari, S., Martino, F., et al. (2017). YAP regulates cell mechanics by controlling focal adhesion assembly. Nat. Commun. *8*, 15321. https://doi.org/10.1038/ncomms15321.
45. Chen, C., Yuan, W., Zhou, Q., Shao, B., Guo, Y., Wang, W., Yang, S., Guo, Y., Zhao, L., Dang, Q., et al. (2021). N6-methyladenosine-induced circ1662 promotes metastasis of colorectal cancer by accelerating YAP1 nuclear localization. Theranostics *11*, 4298–4315. https://doi.org/10.7150/thno.51342.
46. Chen, Y., Ling, Z., Cai, X., Xu, Y., Lv, Z., Man, D., Ge, J., Yu, C., Zhang, D., Zhang, Y., et al. (2022). Activation of YAP1 by N6-Methyladenosine-Modified circCPSF6 Drives Malignancy in Hepatocellular Carcinoma. Cancer Res. *82*, 599–614. https://doi.org/10.1158/0008-5472.Can-21-1628.
47. Mach, J., Atkins, M., Gajewski, K.M., Mottier-Pavie, V., Sansores-Garcia, L., Xie, J., Mills, R.A., Kowalczyk, W., Van Huffel, L., Mills, G.B., and Halder, G. (2018). Modulation of the Hippo pathway and organ growth by RNA processing proteins. Proc. Natl. Acad. Sci. USA *115*, 10684–10689. https://doi.org/10.1073/pnas.1807325115.
48. Howell, M., Borchers, C., and Milgram, S.L. (2004). Heterogeneous Nuclear Ribonuclear Protein U Associates with YAP and Regulates Its Co-activation of Bax Transcription. J. Biol. Chem. *279*, 26300–26306. https://doi.org/10.1074/jbc.M401070200.
49. Jia, Y., Li, H.-Y., Wang, J., Wang, Y., Zhang, P., Ma, N., and Mo, S.-J. (2019). Phosphorylation of 14-3-3ζ links YAP transcriptional activation to hypoxic glycolysis for tumorigenesis. Oncogenesis *8*, 31. https://doi.org/10.1038/s41389-019-0143-1.
50. Moon, S., Kim, W., Kim, S., Kim, Y., Song, Y., Bilousov, O., Kim, J., Lee, T., Cha, B., Kim, M., et al. (2017). Phosphorylation by NLK inhibits YAP-14-3-3-interactions and induces its nuclear localization. EMBO Rep. *18*, 61–71. https://doi.org/10.15252/embr.201642683.
51. Gao, S., Chen, S., Han, D., Wang, Z., Li, M., Han, W., Besschetnova, A., Liu, M., Zhou, F., Barrett, D., et al. (2020). Chromatin binding of FOXA1 is promoted by LSD1-mediated demethylation in prostate cancer. Nat. Genet. *52*, 1011–1017. https://doi.org/10.1038/s41588-020-0681-7.
52. Aveic, S., Pigazzi, M., and Basso, G. (2011). BAG1: The Guardian of Anti-Apoptotic Proteins in Acute Myeloid Leukemia. PLoS One *6*, e26097. https://doi.org/10.1371/journal.pone.0026097.
53. Lecona, E., Rojas, L.A., Bonasio, R., Johnston, A., Fernández-Capetillo, O., and Reinberg, D. (2013). Polycomb protein SCML2 regulates the cell cycle by binding and modulating CDK/CYCLIN/p21 complexes. PLoS Biol. *11*, e1001737. https://doi.org/10.1371/journal.pbio.1001737.
54. Rosenbluh, J., Nijhawan, D., Cox, A.G., Li, X., Neal, J.T., Schafer, E.J., Zack, T.I., Wang, X., Tsherniak, A., Schinzel, A.C., et al. (2012). β-Catenin-driven cancers require a YAP1 transcriptional complex for survival and tumorigenesis. Cell *151*, 1457–1473. https://doi.org/10.1016/j.cell.2012.11.026.
55. Cinar, B., Collak, F.K., Lopez, D., Akgul, S., Mukhopadhyay, N.K., Kilicarslan, M., Gioeli, D.G., and Freeman, M.R. (2011). MST1 is a multifunctional caspase-independent inhibitor of androgenic signaling. Cancer Res. *71*, 4303–4313. https://doi.org/10.1158/0008-5472.Can-10-4532.
56. Cinar, B., Fang, P.K., Lutchman, M., Di Vizio, D., Adam, R.M., Pavlova, N., Rubin, M.A., Yelick, P.C., and Freeman, M.R. (2007). The pro-apoptotic kinase Mst1 and its caspase cleavage products are direct inhibitors of Akt1. EMBO J. *26*, 4523–4534. https://doi.org/10.1038/sj.emboj.7601872.
57. Gao, J., Aksoy, B.A., Dogrusoz, U., Dresdner, G., Gross, B., Sumer, S.O., Sun, Y., Jacobsen, A., Sinha, R., Larsson, E., et al. (2013). Integrative analysis of complex cancer genomics and clinical profiles using the cBioPortal. Sci. Signal. *6*, pl1. https://doi.org/10.1126/scisignal.2004088.

STAR★METHODS

KEY RESOURCES TABLE

REAGENT or RESOURCE	SOURCE	IDENTIFIER
Antibodies		
YAP1 (1A12) Mouse mAb	Cell Signaling Technology (CST)	CST, Cat# 12395; RRID:AB_2797897
YAP1 (D8H1X) XP® Rabbit mAb	Cell Signaling Technology	CST, Cat# 14074; RRID:AB_2650491
SCML2 (G-1) mouse mAb	Santa Cruz Biotechnology (SCBT)	SCBT, Cat# sc-271228; RRID:AB_10613441
SCML2 (C-7) mouse mAb	Santa Cruz Biotechnology	SCBT, Cat# sc-398400; RRID:AB_2938698
Mouse Anti-β-Actin mAb	Millipore Sigma	Sigma-Aldrich, Cat# A2228; RRID:AB_476697
Alexa Fluor™ Plus 488, Goat anti-Mouse IgG, Invitrogen™	Thermo Fisher Scientific	Thermo Fisher Scientific, Cat# A32723; RRID:AB_2633275
Alexa Fluor™ Plus 647, Goat anti-Rabbit IgG, Invitrogen™	Thermo Fisher Scientific	Thermo Fisher Scientific, Cat# A32733; RRID:AB_2633282
Anti-Androgen Receptor (AR), Rabbit mAb	Millipore Sigma	Sigma-Aldrich, Cat# SAB5500006; RRID:AB_2938700
Anti-AR (D6F11) XP® Rabbit mAb	Cell Signaling Technology	CST, Cat# 5153; RRID:AB_10691711
Anti-mouse IgG, HRP-linked Antibody	Cell Signaling Technology	CST, Cat# 7076; RRID:AB_330924
Anti-rabbit IgG, HRP-linked Antibody	Cell Signaling Technology	CST, Cat# 7074; RRID:AB_2099233
YAP/TAZ (D24E4) Rabbit mAb	Cell Signaling Technology	CST, Cat# 8418; RRID:AB_10950494
Ubiquityl-Histone H2A (Lys119) (D27C4) XP® Rabbit mAb	Cell Signaling Technology	CST, Cat# 8240; RRID:AB_10891618
Histone H2A (L88A6) Mouse mAb	Cell Signaling Technology	CST, Cat# 3636; RRID:AB_2118801
Mono-Methyl-Histone H3 (Lys27) (D3R8N) Rabbit mAb	Cell Signaling Technology	CST, Cat# 84932; RRID:AB_2800043
Di-methyl-histone H3 (Lys27) (D18C8) XP® Rabbit mAb	Cell Signaling Technology	CST, Cat# 9728; RRID:AB_1281338
Tri-Methyl-Histone H3 (Lys27) (C36B11) Rabbit mAb	Cell Signaling Technology	CST, Cat# 9733; RRID:AB_2616029
Acetyl-Histone H3 (Lys27) (D5E4) XP® Rabbit mAb	Cell Signaling Technology	CST, Cat# 8173; RRID:AB_10949503
Histone H3 (D1H2) XP® Rabbit mAb	Cell Signaling Technology	CST, Cat# 4499; RRID:AB_10544537
EZH2 (D2C9) XP® Rabbit mAb	Cell Signaling Technology	CST, Cat# 5246; RRID:AB_10694683
Bacterial and virus strains		
BL-21Lys bacteria	Millipore Sigma	Cat# CMC0015
Chemicals, peptides, and recombinant proteins		
GST-YAP1 peptides	Cinar Laboratory	PMID: 28230103
Magnetic Glutathione Sepharose Beads	MilliporeSigma	Cat# G0924
Luminata Forte Western HRP Substrate	MilliporeSigma	Cat# WBLUFO500
Protease Inhibitor Cocktail	Calbiochem	Cat# 539131
DharmoFect-2	Horizon Discovery	Cat# T-2005-01
DharmoFect-3	Horizon Discovery	Cat# T-2003-02
Critical commercial assays		
Duolink Proximity Ligation Assay (PLA) Kit	Millipore Sigma	Cat# DUO92101-1KT
Luciferase Reporter Assay Kit	Promega, Inc	Cat# E397A
Pierce Rabid Gold BCA Protein Assay Kit	Thermo Fisher Scientific	Cat# TB264625
Cell Counting Kit-8 (CCK-8) Assay Kit	Dojindo Molecular Technologies, Inc	Cat# CK04
Experimental models: Cell lines		
LNCaP	American Type Culture Collection	Cat# CRL-1740
C4-2	American Type Culture Collection	Cat# CRL-3314
PC3	American Type Culture Collection	Cat# CRL-1435

(*Continued on next page*)

Continued

REAGENT or RESOURCE	SOURCE	IDENTIFIER
22Rv1	American Type Culture Collection	Cat# CRL-2505
HEK-293T-REx	Bonasio et al.[16]	PMID: 24986859
Deposited data		
MS/MS data available	This paper	https://doi.org/10.5281/zenodo.8286537
SCML2 target genes	Bonasio et al.[16]	PMID: 24986859
YAP1 target Genes	Nardone et al.[44]	PMID: 28504269
Oligonucleotides		
siSCML2 #5 (5′-CCAAACGATCTCAGCAAA-3′)	Bonasio et al.[16]	PMID: 24986859
siSCML2 #6 (5′-CAGTATGTATTGCTACGGTTA-3′)	Bonasio et al.[16]	PMID: 24986859
Non-targeting, small interfering RNA (siRNA)	Horizon Discovery	Cat# D-001810-01-05
SMART Pool ON-TARGETplus SCML2 siRNA	Horizon Discovery	Cat# L-020090-00-0005
SMART Pool ON-TARGETplus YAP1 siRNA	Horizon Discovery	Cat# L-012200-00-0005
Recombinant DNA		
pGEX2-GST Vector	Kuser-Abali et al.[34]	PMID: 28230103
GST-YAP1-WT	Kuser-Abali et al.[34]	PMID: 28230103
GST-YAP1 (2–150)	Kuser-Abali et al.[34]	PMID: 28230103
GST-YAP1 (151–296)	Kuser-Abali et al.[34]	PMID: 28230103
GST-YAP1 (297–504)	Kuser-Abali et al.[34]	PMID: 28230103
HA-Mock Vector	Bonasio et al.[16]	PMID: 24986859
HA-SCML2-WT	Bonasio et al.[16]	PMID: 24986859
HA-SCML2-ΔRBR	Bonasio et al.[16]	PMID: 24986859
pA3-5xTRE-Luc reporter	Al-Mathkour et al.[40]	PMID: 35264657
Software and algorithms		
ImageJ	https://imagej.nih.gov/ij/download.html	ImageJ (RRID:SCR_003070)
GeneMania	https://genemania.org	GeneMANIA (RRID:SCR_005709)
cBioportal	Cerami et al.[42]; Gao et al.[57]	cBioPortal (RRID:SCR_014555)
gProfiler	https://biit.cs.ut.ee/gprofiler/gost	g:Profiler (RRID:SCR_006809)
GraphPad Prism	GraphPad Prism, version 9.2.0, Boston, MA	GraphPad Prism (RRID:SCR_002798)

RESOURCE AVAILABILITY

Lead contact

Further information and requests for resources and reagents should be directed to and will be fulfilled by the lead contact, Bekir Cinar (bcinar@cau.edu).

Materials availability

This study did not generate new unique reagents.

Data and code availability

- The original proteomics data within the paper will be available from the lead contact upon request.
- This paper does not report the original code.
- Any additional information in this paper is available from the lead contact upon request.

EXPERIMENTAL MODEL AND STUDY PARTICIPANT DETAILS

Cell lines

LNCaP (cat# CRL-1740), C4-2 (cat# CRL-3314), 22RV1 (cat# CRL-2505), and PC3 (cat# CRL-1435) cell lines were purchased from American Type Culture Collection (ATCC). The HEK-293T-REx cell line was obtained from the University of Pennsylvania (Dr. Roberto Bonasio).[16] Cells were

grown in RPMI 1640 cell culture medium supplemented with 10% Fetal Bovine Serum (FBS) and 1% penicillin/streptomycin/glutamine and in a cell culture incubator with 5% CO_2. Cell cultures were performed in a certified biosafety level 2 (BL2) mammalian cell culture cabinet.

RNAi gene silencing

Cells (2.5×10^5 per well) were plated in a six-well plate. The next day, culture media was replaced with OptiMEM media before adding the non-targeting, small interfering RNA (siRNA) control (cat# D-001810-01-05), ON-TARGETplus SCML2 siRNA (cat# L-020090-00-0005), and ON-TARGETplus YAP1 siRNA (cat# L-012200-00-0005) were purchased from Horizon Discovery. According to the manufacturer's instructions, the Dharmo*Fect-2* transfection reagent was used to introduce siRNA (50 nM) into cells (cat# T-2005-01, Horizon Discovery). Also, we verified SCML2 knockdown using SCML2 siRNA #5 (5′-CCA AAC GAT CTC CTC AGC AAA-3′) and SCML2 siRNA #6 (5′-CAG TAT GTA TTG CTA CGG TTA-3′), as published,[16] which were obtained from Integrated DNA Technology. After 72h of siRNA transfection, total proteins were extracted from cells on ice using ice-cold cell lysis buffer with a 1X protease inhibitor cocktail (cat# 539131, Calbiochem). Protein and western blotting were conducted as described in the protein analysis section in method details.

METHOD DETAILS

Crosslinking and immunoprecipitation

The IgG and YAP1-antibody crosslinked to Protein A/G Plus Agarose and immunoprecipitation (IP) were conducted according to the manufacturer's protocol (cat# 26147, Pierce, ThermoFisher Scientific). First, nuclear extracts isolated from LNCaP and C4-2 cells were incubated with IgG or AYAP1 antibody crosslinked column. After extensive washing, bound proteins were eluted and analyzed by 8% SDS-PAGE and western blotting according to the published protocol.[33] Next, coimmunoprecipitation (co-IP) was performed in a separate experiment with anti-SCML2, anti-YAP1, or anti-HA-tag antibodies at 4°C overnight according to the established protocol.[34] Briefly, membranes were blocked with blocking (PBS containing 0.1% Tween 20 and 5% non-fat milk) and probed with anti-SCML2, anti-YAP1, anti-AR, anti-beta actin, anti-YAP1/TAZ (Rabbit 1:1000, cat# 8418S, Cell Signaling Technology (CST)), SCML2 (G-1, Mouse, 1:100, cat# sc-271228 or C-7, Mouse, 1:200, cat# sc-398400, Santa Cruz Biotechnology (SCBT)), anti-AR (Rabbit, 1:400, cat# SAB5500006, Millipore Sigma), and anti-beta actin (Mouse, 1:3000, cat# A2228, Millipore Sigma). Then, membranes were exposed to species-specific secondary antibodies (1:2000, anti-mouse, or anti-rabbit cat# 7074 and cat# 7076, CST, respectively) linked to horseradish peroxidase). After each step above, membranes were washed with washing buffer (PBS plus 0.1% Tween 20) three times, 5 min each. Primary and secondary antibody dilutions were prepared in the blocking buffer. Signals were detected using Luminata Forte Western HRP Substrate (cat# WBLUFO500, Millipore Sigma) and the ChemiDoc MP Imaging System (cat# 12003154, Bio-Rad).

Mass spectrometry

Mass spectrometry was conducted at the proteomics core facility at Xavier University of Louisiana, New Orleans, LA, USA. Briefly, LNCaP and C4-2 cells were exposed to DHT and ENZ for 16 h at DCC serum-fed condition, followed by nuclear extracts (NEs) preparation. Next, NEs were incubated with the YAP1 antibody-crosslinked protein A/G agarose columns for 4h at 4°C, followed by extensive washing under stringent conditions. Finally, YAP1-associated proteins were eluted and digested overnight at 37°C with 10 ng/mL sequencing grade modified trypsin (cat# V5111, Promega Inc.) in 10 mM (NH4)HCO3 (cat# A6141, Millipore Sigma). According to the manufacturer's protocol, peptides in the solution were concentrated and purified using ZipTipSCX Pipette Tip (cat# ZTSCXS096, Millipore Sigma). For protein identification, peptides were analyzed by LC-MS/MS (liquid chromatography (LC) coupled with mass spectrometry (MS)).

Protein analysis

Total proteins were extracted from LNCaP or C4-2 cells in ice-cold cell lysis buffer (20 mM HEPES, pH 7.4, 150 mM NaCl, 0.5% NP-40, 1 mM EDTA, and 1X protease inhibitors and phosphatase inhibitor cocktails (cat# 539131, Calbiochem) according to the published study.[33,40] Cytoplasmic and nuclear extracts were isolated using a nuclear extraction kit according to the manufacturer's protocol (cat# 78833, Affymetrix) with modifications. Protein concentration was determined using the Pierce Rapid Gold BCA Protein Assay Kit (cat# TB264625, ThermoFisher Scientific). The proteins were analyzed by 8–10% SDS-PAGE and transferred onto a nitrocellulose membrane (cat# 1620112, 0.2-micron meter, Bio-Rad). Membranes were blocked with PBS containing 0.1% Tween 20 and 5% non-fat milk, followed by incubation with anti-SCML2 (G-1, Mouse, 1:75, cat# sc-271228; C-7, Mouse, 1:200, cat# sc-398400, SCBT), anti-YAP1/TAZ or anti-YAP1 (Rabbit, 1:1000, cat# 8418S, cat# 14074 or mouse 1:100, cat# 12395, CST), anti-AR (Rabbit, 1:400, cat# SAB5500006, Millipore Sigma or Rabbit (1:1000, cat# 5153, CST), anti-H2AK119Ub (1:1000, cat# 8240T, CST), anti-Histone 2A (1:1000, cat# 3636S, CST), anti-H3K27me1 (1:1000, cat# 84932, CST), anti-H3K27me2 (1:1000, cat# 9728, CST), anti-H3K27me3 (1:1000, cat# 9733, CST), anti-H3K27ac (1:1000, cat# 8173, CST), anti-Histone 3 (1:1000, cat# 4499, CST), anti-EZH2 (1:1000, cat:# 5246, CST), and anti-Beta Actin (Mouse, 1:3000, cat# A2228, Millipore Sigma). Secondary antibody anti-mouse IgG, HRP-linked antibody (1:2000, cat# 7076, CST) or anti-rabbit IgG, HRP-linked antibody (1:2000, cat# 7074, CST) was used in protein analysis. Signals were detected using Luminata Forte Western HRP Substrate (cat# WBLUFO500, Millipore Sigma) and the ChemiDoc MP Imaging System (cat# 12003154, Bio-Rad).

GST-pulldown assay

Plasmids expressing pGEX2-GST-YAP1-WT and truncation mutant of GST-YAP1 (2–150), GST-YAP1 (151–296), or GST-YAP1 (297–504) were described previously.[34] GST vector and GST-YAP1 fusion peptides were induced in BL-21Lys bacteria (cat# CMC0015, Millipore Sigma) in 1 mM IPTG for 4h at 37°C. Recombinant GST vector and GST-YAP1 fusion peptides were solubilized in NETN buffer (1% NP-40, 20 mM Tris-HCl, pH 8.0, 100 mM NaCl, and 1 mM EDTA). GST fusion peptides were purified by affinity chromatography on Magnetic Glutathione Sepharose beads (cat# G0924, Millipore Sigma) and stored in PBS at 4°C until use. Recombinant, purified GST control or GST-YAP1 mutant peptides mixed with total lysates isolated from LNCaP cells grown in serum-fed conditions were incubated for 2h at 4°C for constant rotation. The lysates from LNCaP cells were the source of SCML2. After extensive washing of unbound proteins, bound protein was eluted and analyzed by 8% SDS–PAGE. Coomassie blue staining visualized the GST-only or GST-YAP1 fusion peptides. Western blots visualize the bound SCML2 protein.

Proximity ligation assay

Duolink proximity ligation assay (PLA) combined with confocal microscopy was conducted to assess the interaction between YAP1 and SCML2 protein with the cell according to the manufacturer's instruction (cat# DUO92101-1KT, Millipore Sigma). Briefly, cells were seeded in an eight-chamber slide (1×10^4 cells/well). After androgen depletion, cells were treated with vehicle, dihydrotestosterone (DHT, 10 nM), and DHT plus enzalutamide (20 μM) in dextran-coated charcoal (DCC) stripped serum-medium for 16h. The chambers were washed with phosphate-buffered saline (PBS) three times, 5 min each, and then cells were fixed with 4% paraformaldehyde (PFA) for 20 min, followed by BPS washing as above. Cells were then permeabilized with 0.3% Triton X-100 for 10 min and then PBS washing. Cells were blocked with 1X blocking solution for 1 h at 37°C in a humidified chamber. Note that it is critical to vortex the blocking solution before using it. After blocking, cells were co-incubated with primary antibodies overnight at 4°C. Primary antibodies used in PLA are anti-YAP1 (Rabbit, 1:200, cat# 8418S, CST) and anti-SCML2 (G-1 or C-7 SCBT). The chambers were washed in 1X Buffer A twice, 5 min each. The cells were then incubated with probes for 1h at 37°C, followed by washing 1X Buffer A twice, 5 min each. Then, the probe ligation step was completed for 30 min at 37°C, followed by washing with 1X Buffer A twice, 5 min each. Next, the slides were incubated with an amplification solution for 1h and 40 min at room temperature to amplify the signal. Then, the slides were washed 1X Buffer B at room temperature, 10 min each, and then 0.01x Buffer B for 1 min. After drying slides for 1h, coverslips were mounted using mounting media with DAPI (4′,6-diamidino-2-phenylindole dihydrochloride) for 30–60 min. Slides can be stored at −20°C for up to 1 year. Images were captured using confocal microscopy (Zeiss, LSM 700 Confocal Microscope) with 40X or 60X magnification.

Immunofluorescence microscopy

Cells (1×10^4 or 2×10^4 cells per in 4 or 8-chamber, respectively) were seeded at 70% confluent. After serum depletion overnight, cells were treated with vehicle (0.01% ethanol or DMSO, 10 nm DHT, or DHT plus 20 μM enzalutamide for 16h. Cells were washed with PBS three times, 5 min each, then fixed with 4% PFA for 15 min, followed by PBS washing. Next, cells were permeabilized with 0.3% Triton X-100 prepared in PBS for 3–5 min, followed by PBS washing. Next, cells were incubated with 2% BSA and 0.3% Triton X-100 prepared in PBS for 1h at room temperature to block non-specific binding, followed by PBS washing. Cells were incubated with anti-YAP1 (Rabbit 1:100, cat# 8418S, CST) or anti-SCML2 (C-7, Mouse, cat#sc-398400 1:30, SCBT) primary antibody overnight at 4°C, followed by PBS washing. Cells were incubated with secondary antibody AlexaFlour 488 conjugated anti-mouse IgG (1:500, cat# A32723, ThermoFisher Scientific) or AlexaFlour 647 conjugated anti-rabbit IgG (1:500, cat# A32733, ThermoFisher Scientific) for 1h at room temperature to visualize YAP1 or SCML2 signals, followed by PBS washing. Lastly, chambers were removed, and coverslips were mounted with Vectashield with DAPI. Images were captured by confocal microscopy (Zeiss LSM 700 Confocal Microscope) with 40X or 63X magnification.

RNA isolation and quantitative PCR

Total RNA from LNCaP and C4-2 cells were extracted using TriAzol reagent according to the manufacturer's instruction (cat# 15596026, Life Technologies). Quantitative PCR was conducted using the GoTaq 1-Step RT-qPCR System (cat# A6020, Promega) and Real-Time PCR instrument (cat# 185520, CFX Connect Real-Time PCR Detection System, Bio-Rad) to amplify SCML2 transcripts using the primer set (Fv: 5′-CCA GTG CAT CCC TCA GAT TT-3′ and Rv: 5′-GAG CCC TGA AGA AGA ACC ATA C-3′). In addition, the primer set used to amplify 18S RNA as an internal control in qPCR was reported in a published study.[40]

Luciferase reporter assay

Cells (2.5×10^5 per well) were plated in a six-well plate. The following day, cells were co-transfected with pA3-5xTRE-Luc vector and mock (scramble), YAP1, or SCML2 siRNA using Dharmo*Fect-2* transfection reagents according to the manufacturer's instruction and published study.[40] The construction of the pA3-5xTRE-Luc promoter reporter vector was described.[40] Luciferase reporter assay was conducted per the manufacturer's instruction (cat# E397A, Promega) at 72h post-transfection. Relative Luciferase Units (RLUs) in a 96-well plate (Dynex) with a 2-s measurement delay, followed by a 10-s measurement, were measured using LUMIstar OPTIMA Microplate Luminometer (BMG LabTech). The data were presented as luciferase activity after normalizing RLUs to total protein.

Cell growth assay

Cell growth was assessed in a 96-well culture plate using the cell counting kit-8 (CCK-8) assay system according to the manufacturer's instructions (cat# CK04, Dojindo). Briefly, LNCaP or C4-2 cells were seeded in 96-well cell culture plate in triplicates and transiently transfected with mock (scramble) or SMART-pool of SCML2 siRNA for 24h in serum-fed conditions, followed by treatment with vehicle control, androgen, and enzalutamide in androgen-depleted DCC-fed serum for 48h. At 72h post-transfection, cells were exposed to CCK-8 reagent for up to 4h to measure cell growth. Cell growth was also evaluated using a standard crystal violet assay as a complementary approach under the above conditions.

QUANTIFICATION AND STATISTICAL ANALYSIS

Data analysis

Pan-cancer gene expression dataset from prostate adenocarcinoma (PRAD) patients were obtained from The Cancer Genome Atlas (TCGA). Batch-normalized Illumina RNAseq V2 data from 494 patients were accessed via the cBioPortal (RRID: SCR_014555).[42,57] cBioportal co-expression tools (Pearson correlation = 0.29, p = 2.46e^{-}11). Microsoft Excel (RRID: SCR_016137) was used to perform a correlation analysis of SCML2 and STK4 mRNA data, construct graphs, and identify the YAP1 and SCML2 overlapping target genes. Protein networks were constructed using GeneMania (RRID: SCR_005709) web tool. ImageJ was employed to quantify micrographs (RRID: SCR_003070). Gene Ontology (GO) analysis was conducted using the g:Profiler web portal. (RRID: SCR_006809). GraphPad Prism (RRID: SCR_002798) was used to construct heatmaps. A *t*-test with Microsoft Excel was conducted to determine the significance between the control and test samples. A p value set to equal to or less than 0.05 was considered significant.